JOURNAL OF CATALYSIS 111, 302–316 (1988)

Oxidative Dimerization of Methane over Sodium-Promoted Calcium Oxide

CHIU-HSUN LIN, JI-XIANG WANG, AND JACK H. LUNSFORD

Department of Chemistry, Texas A&M University, College Station, Texas 77843

Received September 8, 1987; revised November 17, 1987

Sodium-promoted calcium oxides are active and selective catalysts for the partial oxidation of methane to ethane and ethylene using molecular oxygen as an oxidant. In a conventional fixed-bed flow reactor, operating at atmospheric pressure, a 45% C_2 (sum of ethane and ethylene) selectivity was achieved at a 33% methane conversion over 2.0 g of 15 wt% Na/CaO catalyst at 725°C with a gas mixture of $CH_4/O_2 = 2$. The other products were CO, CO_2, and H_2. EPR results indicated that $[Na^+O^-]$ centers in Na/CaO are responsible for the catalytic production of $CH_3\cdot$ from methane via hydrogen atom abstraction. These $CH_3\cdot$ radicals dimerize, primarily in the gas phase, to form C_2H_6, which further oxidizes to C_2H_4. Increasing temperatures reverse the gas-phase equilibrium $CH_3\cdot + O_2 \rightleftarrows CH_3O_2\cdot$ to produce more $CH_3\cdot$ and increase the C_2 selectivity. The $CH_3O_2\cdot$ eventually is converted to carbon oxides under the reaction conditions employed; therefore, increasing O_2 pressures decrease the C_2 selectivity. There is evidence that $CH_3O_2\cdot$ in the presence of C_2H_6 initiates a chain reaction that enhances the methane conversion. The addition of Na^+ to CaO also reduces the surface area of the catalysts, thus minimizing a nonselective oxidation pathway via surface methoxide intermediates.

INTRODUCTION

Methane, or natural gas, is present in vast, proven reserves worldwide; however, most of the production is flared, with less than half being used either as a source of energy or as chemicals. As a result of high molecular stability, it is very difficult to activate the carbon–hydrogen bonds in methane in a selective manner. Nevertheless, considerable progress has been made in the development of catalysts for the oxidative dimerization of methane. The more promising catalysts include certain members of the lanthanide oxide series (*1*, *2*), as well as a number of metal oxides promoted with Group IA ions (*3–9*).

Recently, we reported that lithium-promoted magnesium oxide is an effective catalyst for the conversion of methane into ethane and ethylene using oxygen as the oxidant (*10*). In this promoted oxide, $[Li^+O^-]$ centers were found, and these are believed to be the active sites for the reaction. Other combinations of Group IA/Group IIA oxides were then screened for activity, and it was found that sodium-promoted calcium oxide (Na/CaO) was as active and selective as Li/MgO. EPR results indicated that Na/CaO contains the analogous type of O^- center, i.e., $[Na^+O^-]$ (*11*). In this paper the catalytic properties of the Na/CaO system are described in more detail, and by comparing these results with those of Li/MgO, we hope to provide a more comprehensive picture of the active site and the mechanism for the oxidative dimerization of methane.

EXPERIMENTAL

Catalyst Preparation and Reagents

The same slurry method used for preparing the Li/MgO (*10*) was employed for all of the Na/CaO catalysts. That is, CaO was added to a solution containing the appropriate sodium salt and the resulting slurry was boiled several hours, which converted the calcium oxide to the hydroxide. The material in the form of a thick paste was dried

0021-9517/88 $3.00

overnight in air at 120°C. The materials were the following: Aldrich CaO (Gold Label, >99.999%), Malinckrodt Na_2CO_3 and $Na_2C_2O_4$ (Primary Standard, >99.5%), Fisher $NaNO_3$ (Certified ACS, >99.0%). The weight percentage of promoter is defined as the ratio of Na to the sum of Na plus CaO. A low-surface-area CaO was prepared by calcining the $Ca(OH)_2$ at 900°C for 24 h. Catalysts of 20–40 mesh with an apparent density of 0.8 g liter^{-2} were used in all runs. Methane (>99.97%), oxygen (>99.6%), and ethane (>99.0%) were obtained from Matheson Gas and helium (>99.995%) was from Airco. No further purification was attempted.

Catalyst Pretreatment and Product Distribution

A fixed-bed fused-quartz reactor, described previously (*10*), was operated at atmospheric pressure. The hydroxides were treated in the reactor at 550°C for 1 h under an oxygen flow of 0.83 ml s^{-1}. A reacting gas mixture (methane and oxygen) was then introduced, and the temperature of the system was increased to the desired level. A period of 10 h was required for the catalyst to reach steady state, and normally the activity was determined after this period. The total flow rate of the reactant gas mixture was 0.92 ml s^{-1} except when measuring the effect of contact time. In most experiments helium was used as a diluent to achieve atmospheric pressure; when the production of H_2 was examined, argon was the diluent.

The GC method used to analyze the products has been described previously (*12*). In addition to major products (C_2H_4, C_2H_6, CO, and CO_2 and H_2), a small amount (<1%) of C_3H_6, C_3H_8, CH_3OH, and HCHO was also detected, but these components were neglected in the calculations. No attempt was made to analyze CH_3O_2H and H_2O. Typically, a 97% carbon mass balance was achieved. The surface areas of the used catalysts were measured by the BET method using krypton as the adsorbate at −196°C. The estimated error is ±0.5 m^2 g^{-1}.

Catalyst Characterization

The XPS spectra of the used catalysts were obtained with a Kratos XSAM-800 spectrometer with Mg $K\alpha$ X rays (1100 eV). The concentration in atom percent was calculated from the relationship $(A_i/S_i)/(\Sigma A_i/S_i) \times 100$, where A_i and S_i are the peak area and the atomic sensitivity factor, respectively, of species i. A physical mixture of a sodium salt and CaO was also tested for comparison purpose. The results reported here have ±20% uncertainty. In these experiments, only the elements oxygen, sodium, calcium, carbon, and nitrogen, were scanned.

The EPR spectra of $[Na^+O^-]$ centers in the catalysts were measured at −196°C using a Varian E-6S EPR spectrometer. The same reactor and experimental method were used as described previously for Li/MgO (*10*). The g values are reported relative to a phosphorus-doped silicon standard with $g = 1.9987$.

The inductively coupled plasma (ICP) method was used to analyze the sodium content of the fresh and used catalysts. The catalysts were digested in a 3 N HCl solution, and the analysis was performed on the resulting solution. The X-ray powder diffraction pattern of a used Na/CaO catalyst was also obtained to determine whether there was any Na_2CO_3 phase present.

RESULTS

Variation in Activity and Selectivity with Time

The change in catalytic activity during the reaction at 725°C was examined using 1.0 g of 15% Na_2CO_3/CaO, and the results are shown in Fig. 1. In this experiment, the catalyst was treated as described in the previous section, except that once the temperature reached 725°C, the analysis was started immediately. Carbon balance calculations (110% and 105% for the first two

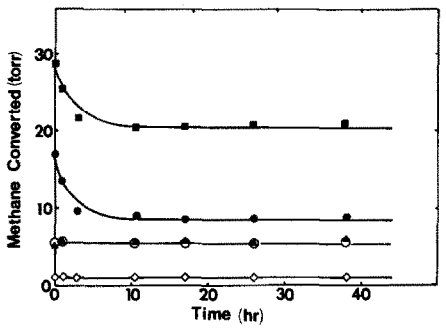

FIG. 1. Effect of time on stream on the amount of methane converted and products formed over 1.0 g of 15% Na/CaO at 725°C: ■, total; ○, to C_2H_4; ▲, to C_2H_6; ●, to CO_2; ◇, to CO. 76 Torr of CH_4 and 38 Torr of O_2 were used at a flow rate of 0.92 ml s^{-1}.

data points, and 99% for the rest) suggest that during the early part of the experiment some of the CO_2 may have resulted from decomposition of the Na_2CO_3 phase or carbonate species formed below 725°C.

The total amount of CH_4 converted decreased from 28.6 to 20.7 Torr, with no apparent decrease in C_2 production for the first 10 h; thereafter, constant activity was observed. The decrease in CO_2 formation resulted in an increase in C_2 selectivity from 37 to 53%. This, in turn, increased the C_2 yield from 12.4 to 14.2%. ICP analysis showed that there was no significant loss in Na^+ content of the used catalyst. The remarkable stability of this catalyst is attributed to the fact that the temperature was never greater than 725°C.

Effect of the Sodium Concentration

To investigate the effects of Na^+ concentration on catalytic activity and selectivity, reactions were carried out at 675°C with 1.0-g samples of catalysts of different Na^+ content. Low-surface-area CaO and pure Na_2CO_3 were also examined. Because of its low surface area, 2.0 g of Na_2CO_3 was used. The variations of activity and selectivity as a function of Na^+ content are shown in Fig. 2, together with the change in concentration of $[Na^+O^-]$ and surface area. Without the catalyst there was no reaction below 725°C.

As clearly shown in Fig. 2, pure CaO and 0.4% Na/CaO produced mainly C_1 compounds (CO + CO_2), while C_2 compounds (C_2H_6 + C_2H_4) were the major products after a larger amount of Na^+ (>3 wt%) had been added. Among the catalysts studied, 15% Na/CaO was the most active, but the catalyst containing 32% Na^+ was the most selective in the formation of C_2 compounds (ca. 80%). Pure Na_2CO_3, which is represented in Fig. 2 as 43% Na content, was not very active and produced mostly C_1 compounds.

In Na/CaO, an EPR signal with $g_\perp$ = 2.123 has been assigned to the $[Na^+O^-]$ center (see below), and its intensity indeed increased with Na content. The g value is essentially the same as that observed previously in a sodium-promoted CaO single crystal (*13*). The absolute spin concentration of $[Na^+O^-]$ in a 15% Na/CaO was ca. 1.5×10^{16} centers per gram.

The surface areas of the used catalysts decreased with increasing Na content. For example, the surface area of CaO was 3.3 m^2/g, but that of 15% Na/CaO was about 0.9 m^2/g. As the surface area decreased, the pressure of C_1 compounds in the product

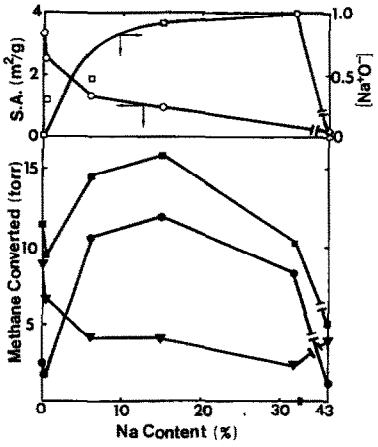

FIG. 2. Effect of Na^+ concentration on $[Na^+O^-]$ concentration (□), surface area (○), amount of CH_4 converted (■, total; ●, C_2; ▼, C_1) over Na/CaO: 1.0 g of catalyst, 300 Torr of CH_4, 20 Torr of O_2, flow rate = 0.92 ml s^{-1}, T = 675°C.

TABLE 1

Counterion Effect on Catalytic Activity and Selectivity[a]

Promoter	Surface area (m^2/g)	Conversion (%)		Selectivity (%)				$[Na^+O^-]^b$
		CH_4	O_2	CO	CO_2	C_2H_4	C_2H_6	
Na_2CO_3	1.0	28	63	2.9	48	24	26	1
$Na_2C_2O_4$	3.5	23	52	4	44	24	27	—
$NaNO_3$	2.6	17	31	5	36	28	31	1.3

[a] 1.0 g of catalyst, 15 wt% in Na^+, promoter decomposed at 725°C; 76 Torr of CH_4 and 38 Torr of O_2, reaction run at 725°C, total flow rate of 0.92 ml s^{-1}.

[b] Relative intensity.

stream also decreased significantly, from 8.94 to 2.08 Torr.

Over Na/CaO it appears that the presence of $[Na^+O^-]$ centers is necessary for this promoted oxide to be an active and selective catalyst. This can be deduced from the data in Fig. 2. As the surface area of the catalysts was reduced (with respect to CaO) by addition of Na^+, the amount of CH_4 converted per unit surface area actually increased from 3.5 to 20.5 Torr/m^2. Apparently, some new active site, presumably $[Na^+O^-]$, was being formed on the catalyst surface. The only exception was the sample that contained 0.4% Na. In this case some $[Na^+O^-]$ was detected, although the specific activity and C_2 selectivity were similar to those of pure CaO.

To test independently the effect of surface area on C_2 selectivity, two CaO samples of different surface areas were prepared (6 and 3 m^2/g). At a comparable conversion (24%), the lower-surface-area CaO gave 16% C_2 selectivity compared with 8% for the higher-area catalyst. Thus, in part, the improved C_2 selectivity upon addition of Na is related to the decrease in CaO surface area.

Effect of Counterion

Catalysts promoted with different Na salts were prepared to test the counterion effect, and the results are given in Table 1. There was a significant variation in catalytic activity and selectivity with different counterions. When $NaNO_3$ was used to introduce the promoter, the catalyst was only 60% as active as its Na_2CO_3 counterpart, although it is the most selective one (59% C_2 selectivity) among the catalysts studied. The C_2H_4-to-C_2H_6 ratio of all three catalysts was 0.9.

It is interesting to note that the least active $NaNO_3$/CaO contained 30% more $[Na^+O^-]$ sites than the more active Na_2CO_3/CaO. XPS results on $NaNO_3$/CaO (Table 2) indicate that by comparison with a physical mixture there was a significant change in the surface composition in the used catalyst. After use, the surface Na^+ concentration increased from 1.9 to 3.3%, and the Ca^{2+} concentration decreased from 15.7 to 10.6%. Furthermore, there was no observable nitrogen peak in the XPS spectra, and, instead, the surface was replenished with carbonaceous and carbonate species (the concentration increased by 7.95 and 4.82%, respectively).

Effect of Methane-to-Oxygen Ratio on Maximum C_2 Yields

To obtain the optimum condition for maximum C_2 yield for Na/CaO, experiments using 2.0 g of 6 and 15% Na/CaO were carried out with different reactant gas compositions. Table 3 summarizes results at 725°C. A C_2 yield as high as 15% (runs 1 and 5) was obtained over these catalysts.

With a CH_4-to-O_2 ratio of 2 the CH_4 conversion and C_2 selectivity (runs 1 and 5)

TABLE 2

Surface Atomic Concentration for Na/CaO Catalysts

Catalyst	Concentration (%)					
	O	Na	Ca	C		N
				Carbon	CO_3^{2-}	
6% Na_2CO_3/CaO						
Mixture[a]	38.7	0.6	17.4	31.5	11.7	—
Used	40.6	1.0	18.8	28.6	10.5	—
15% Na_2CO_3/CaO						
Used	40.0	3.3	16.6	24.2	15.9	—
15% $NaNO_3$/CaO						
Mixture	41.8	1.9	15.7	28.9	9.9	1.7
Used	34.6	3.3	10.6	36.8	14.8	0

[a] Physical mixture of the two components.

were generally good. The CH_4 conversion was about 34% with a C_2 selectivity of 44%, and approximately 85% of the O_2 was consumed. Similar results were obtained when the absolute pressures of CH_4 and O_2 were increased, provided their ratios were kept at approximately 2 (runs 4 and 8). A higher CH_4-to-O_2 ratio led to better C_2 selectivity but lower CH_4 conversion (runs 2 and 6), while a lower CH_4-to-O_2 ratio led to higher CH_4 conversion but poorer C_2 selectivity (runs 3 and 7). A much higher C_2 selectivity of 80% was obtained when the same reactant gases used to obtain the data in Fig. 2 were fed over 1.0 g of 15% Na/CaO at 675°C, although the conversion decreased to 8.2%.

The effect of varying the CH_4-to-O_2 ratio

TABLE 3

Effect of CH_4/O_2 Ratio on Catalytic Activity and Selectivity[a]

	6% Na/CaO				15% Na/CaO			
Run No.:	1	2	3	4	5	6	7	8
Reactant/diluent (Torr)								
He	642	607	534	442	644	609	534	427
CH_4	76.8	114	112	203	78.2	113	114	216
O_2	40.7	39.3	114	115	37.7	38.3	112	117
Product (Torr)								
CO_2	16.1	13.4	38.7	39.5	14.0	14	26.3	37.4
CO	0.62	1.14	2.87	4.89	0.72	0.99	2.4	4.1
C_2H_4	3.60	4.27	4.48	8.95	3.12	3.93	5.30	8.10
C_2H_6	2.53	3.73	3.55	6.25	2.97	4.02	3.51	7.10
Conversion (%)	35.9	25.5	45.5	32.1	32.7	26.1	38.7	28.9
C_2 Selectivity (%)	42.3	52.4	27.9	40.6	45.4	51.5	38.3	42.2
C_2 Yield (%)[b]	15.2	13.3	12.7	13.0	14.8	13.4	14.8	12.2

[a] 2.0 g of catalyst; reaction run at 725°C; total flow rate of 0.92 ml s^{-1}.

[b] Yield is defined as conversion multiplied by selectivity.

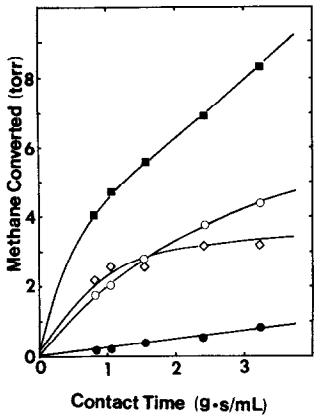

FIG. 3. Effect of contact time on the amount of CH_4 converted over 2.0 g of 15% Na/CaO at 625°C: ■, total; ●, to C_2H_4; ○, to C_2H_6; ◇, to C_1. 300 Torr of CH_4 and 20 Torr of O_2 were used.

over Na/CaO was similar to that reported for Li/MgO, and the amount of C_2 produced over both catalysts was also comparable. The Na/CaO catalysts, likewise, are among the most active and selective systems reported in the recent literature for partial oxidation of methane.

In several catalytic experiments the product stream was analyzed for H_2, and it was found, for example, that under the conditions of run 5 the partial pressure of H_2 was 2.5 Torr. As the reaction temperature was decreased the partial pressure of H_2 increased somewhat, and at 675°C under the same flow conditions the H_2 partial pressure was 2.8 Torr. Several reactions could account for the formation of H_2; however, it is significant to note that at the higher temperatures the partial pressures of H_2, H_2O, CO, and CO_2 approach those expected from the water-gas shift reaction at equilibrium.

Kinetic Measurements

To obtain kinetic parameters for Na/CaO under differential conditions, all runs were carried out at 625°C, except when the temperature effect was measured. The conversions of methane were always kept below 5%, but the oxygen consumption, in a few cases, was as high as 30% since only 20 Torr of O_2 was used to achieve good C_2 selectivity.

The contact time profile is depicted in Fig. 3, in which the contact time is defined as the weight of catalyst divided by the total flow rate of reactant gases. Although the sum of all the product pressures and the partial pressures of C_2 compounds increased with contact time, the amount of C_1 compounds formed became nearly constant at contact times above 1.6 g s ml^{-1}. Contrary to the results with Li/MgO (*9*), at longer contact times (above 1.6 g s ml^{-1}), Na/CaO produced more C_2 compounds than carbon oxides, but this phenomenon disappeared at higher temperatures.

Furthermore, if one were to extrapolate the linear region of the curve of CH_4 converted to zero contact time, the intercept would not be zero. The same observation was made with 4.0 g of catalyst. The C_2H_4 production, however, decreased and approached zero as the contact time decreased, indicating that ethylene is a product of a secondary reaction from ethane.

The reasons for the unusual activity at short contact times and the higher C_2 selectivity at longer contact times over Na/CaO are not clear at the present. At low flow rates a model of a laminar layer of gas "film" enriched with $CH_3\cdot$ radicals (thus, higher coupling rate) best accounts for the formation of higher concentrations of C_2 at a longer contact time. Higher flow rates and temperatures result in turbulent flow and more rapid diffusion, respectively, which allows the mixing of two adjacent layers of fluids. A lower O_2 concentration in the film may be another reason for the formation of more C_2, although the overall reaction is not controlled by the O_2 diffusion process since the total amount of CH_4 converted changed linearly over a wide range of contact times. It is our belief that in addition to the $CH_3\cdot$ radicals produced at the catalyst surface, a small but significant amount of $CH_3\cdot$ radicals are generated through gas-phase chain reactions (see below). This het-

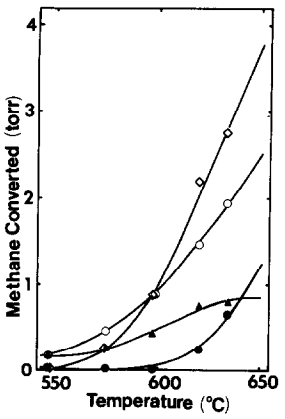

FIG. 4. Effect of temperature on the amount of CH_4 converted over 1.0 g of 15% Na/CaO: ●, to C_2H_4; ◇, C_2H_6 formed; ○, to CO_2; ▲, to CO. 300 Torr of CH_4 and 20 Torr of O_2 were used at a flow rate of 0.92 ml s^{-1}.

erogeneous–homogeneous nature of the catalytic reaction may explain the abnormal behavior at near-zero contact times, as noted in Fig. 3.

The variation of product pressure with temperature is shown in Fig. 4. Except for CO , which ceased to increase above 640°C, the pressures of the other products increased exponentially with temperature. The apparent activation energy for the overall conversion of CH_4 was 49.9 ± 2.5 kcal mol^{-1} over the temperature range 548 to 640°C. This value is close to the value of 55 kcal mol^{-1} observed for Li/MgO under similar conditions (*10*). However, it is considerably greater than the activation energy for the partial oxidation of CH_4 over precious metals or simple and complex metal oxides, which generally have values between 20 and 30 kcal mol^{-1} (*14*).

If the activation energies are determined separately for the formation of C_2 and C_1 compounds, the values are 68.8 and 34.5 kcal mol^{-1}, respectively. The large difference between the two values reflects the higher C_2 selectivity at the elevated temperature. The C_2 selectivity increased from 0% at 548°C to 62% at 638°C. Likewise, better C_2 yields were obtained at higher temperatures since the CH_4 conversion also increased with temperature. It should be noted that the C_2 selectivity decreased above 675°C due to further oxidation of C_2H_4 and C_2H_6.

To explore the reaction further, the conversion of CH_4 to each product was determined as a function of the pressure of each reactant. The effect of varying the CH_4 pressure is shown in Fig. 5. The increase in conversion corresponds to a reaction order of 0.3 with respect to CH_4. Below 100 Torr of CH_4, the formation of both C_2 and C_1 increased with increasing CH_4 pressure, but above 100 Torr of CH_4, C_1 formation did not increase appreciably. The C_2H_6-to-C_2H_4 and CO_2-to-CO ratios were ca. 5/7 and 7/3, respectively, under these reaction conditions.

Figure 6 depicts the interesting effect of O_2 pressure on the reaction. The amount of CH_4 converted increased steeply to a maximum at 60 Torr of O_2, then gradually decreased and became constant at around 185 Torr of O_2. The number of $[Na^+O^-]$ centers, as determined by EPR in a separate experiment, increased linearly with O_2 pressure. The formation of C_2 also increased rapidly with O_2 pressure up to 20 Torr, but fell off rapidly with further increase in O_2 pressure. The formation of C_2H_4 was similar to that of C_2H_6 with re-

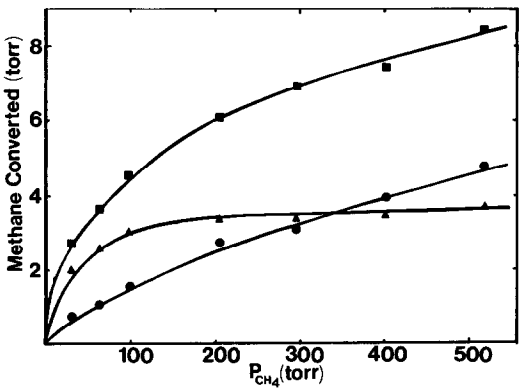

FIG. 5. Effect of methane pressure on the amount of CH_4 converted over 2.0 g of 15% Na/CaO at 625°C: ■, total; ●, to C_2; ▲, to C_1. 20 Torr of O_2 was used at a flow rate of 0.92 ml s^{-1}.

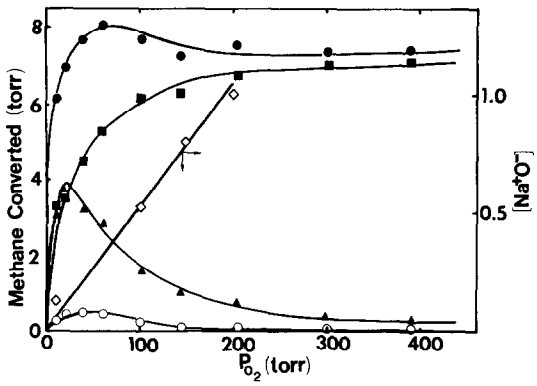

FIG. 6. Effect of oxygen pressure on the amount of CH_4 converted and $[Na^+O^-]$ concentration over 2.0 g of 15% Na/CaO at 625°C: ●, total; ▲, to C_2; ■, to C_1; ○, to C_2H_4; ◇, $[Na^+O^-]$. 300 Torr of CH_4 was used at a flow rate of 0.92 ml s^{-1}.

spect to O_2 pressure, although the maximum in the C_2H_4 curve was shifted to around 50 Torr. The latter observation, again, indicates that C_2H_4 is a secondary product from C_2H_6. At 625°C and at a conversion of ca. 2 to 3%, the C_2H_6-to-C_2H_4 ratio was about 7/10, and that of CO_2 to CO was 7/2.

The presence of small amounts of higher hydrocarbons, especially C_2H_6, has long been known to increase the CH_3OH yield or lower the reaction temperature during the catalytic partial oxidation of CH_4 (*15, 16*). To test this effect, 3 Torr of C_2H_6 mixed with 300 Torr of CH_4 and 185 Torr of O_2 (a composition beyond the maximum in CH_4 conversion of Fig. 6) were fed over the catalyst. The CH_4 converted increased to 8.38 Torr, which is greater than the 8.09 Torr observed at the maximum.

Origin of the Carbon Oxides

To determine whether the CO and CO_2 were produced through further oxidation of C_2H_6 and C_2H_4 or through CH_4 via another pathway, the C_2H_6 and C_2H_4 were introduced either separately or with CH_4 over the catalyst. In the first three runs in Table 4, CH_4, C_2H_6, and C_2H_4 were used separately as reactants, while CH_4 and C_2H_6 were used in run 4. The C_2H_6 and C_2H_4 pressures chosen for runs 2 and 3 were based on the pressures of products obtained in run 1. Runs 2 and 3 show that C_2 compounds, when reacting alone, produced less than half the CO and CO_2 obtained when CH_4 was the reactant (1.26 and 0.79 Torr, respectively, compared with 2.21 Torr from CH_4). The presence of C_2H_6 did not significantly increase the production of carbon oxides in run 4; i.e., a similar amount of C_1 was found in both runs 1 and 4 (2.21 and 2.32 Torr). This suggests that C_2H_6, even when present in appreciable quantities, cannot compete very effectively with a large excess of CH_4 for the same O^- center to produce C_2H_4 and ultimately CO_2. The results of run 4 further support this concept in that when both reactants were present, less C_2H_4 (0.48 Torr) was found than in run 2 (0.61 Torr) in which C_2H_6 was the only product. By comparing data in runs 1 and 3, similar arguments can be used to show that CO and CO_2 were not derived from C_2H_4. Based on the above consideration we conclude that the primary route to produce C_1 is not the further oxidation of C_2, at least at temperatures less than 675°C.

TABLE 4

Reactivity of Methane and Ethane over Na/CaO[a]

	Run No.			
	1	2	3	4
Reactant (Torr)				
CH_4	306.3	—	—	300.4
C_2H_6	—	2.82	—	2.76
C_2H_4	—	—	1.1	—
O_2	21.5	21.4	20.8	21.3
Product (Torr)				
CO_2	1.54	0.94	0.22	1.62
CO	0.67	0.32	0.57	0.69
CH_4	(298.7)	—	—	(291.6)
C_2H_6	1.33	(1.74)	—	(3.53)
C_2H_4	0.18	0.61	(0.71)	0.48

[a] 1.0 g of solid decomposed at 725°C; reaction run at 625°C; total flow rate of 0.92 ml s^{-1}.

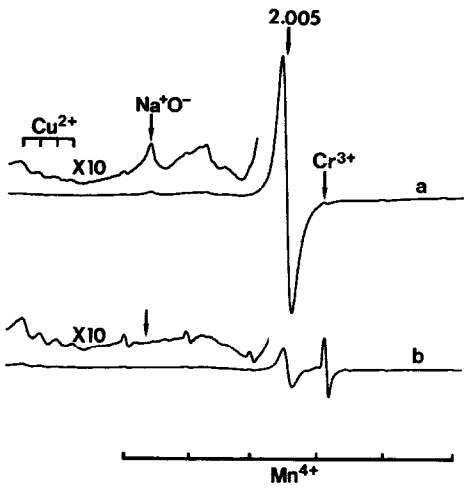

FIG. 7. EPR spectra of samples heated at 650°C for 1 h followed by rapid quenching to −196°C: (a) 15% Na/CaO used catalyst heated in 170 Torr of O_2; (b) pure CaO (a fresh sample) heated in 190 Torr of O_2.

Characterization of Catalysts

X-Ray powder diffraction patterns of 15% Na/CaO catalysts used at 725°C indicated that a considerable amount of Na_2CO_3 had decomposed, although some was still present. There was no evidence for the Na_2O phase, but NaOH probably was present. In addition to CaO, small amounts of $CaCO_3$ and $Ca(OH)_2$ were also found in the used catalysts.

XPS results indicate that the surface composition of the 6% used Na/CaO catalyst was similar to the composition of the physical mixture. The Na phase spread out somewhat on the surface in the used catalysts, as indicated by the increase in the Na^+ signal (Table 2). This was especially true when the more easily melted material, $NaNO_3$ (mp 308°C), was used as the promoter, and it may contribute to the reduction of the Ca^{2+} signal (and therefore exposed CaO surface). In addition, $NaNO_3$ decomposed and formed a layer of less active Na_2CO_3/Na_2O on the surface during the reaction, as was evident by the absence of the nitrogen peak and the increase in carbonate signal intensity. This newly formed Na_2CO_3/Na_2O prevented O^- centers from being exposed to the reactant gases, and resulted in a decrease in the activity of $NaNO_3$/CaO (Table 1).

Preliminary EPR experiments on the Na/CaO catalysts were also carried out, and the spectrum of a 15% used sample is compared with that of pure CaO in Fig. 7. When the promoted sample was heated at high temperature in O_2 and quenched to 77 K, a signal with $g_\perp = 2.123$ was observed (spectrum a). The g value is in exact agreement with that of $[Na^+O^-]$ observed in a single crystal (*13*). A more intense signal was obtained by UV irradiation of the catalyst at 77 K. The rather symmetric peak at $g = 2.005$ may be the spectrum of F-type centers. There is an unidentified series of peaks centered at 2.089.

When the sample was cooled slowly from high temperature, only a trace amount of $[Na^+O^-]$ was present. As with the $[Li^+O^-]$ center in the Li/MgO catalyst, the presence of O_2 during the thermal treatment of Na/CaO promoted the formation of $[Na^+O^-]$ centers, and its signal intensity increased linearly with O_2 pressure up to 200 Torr (Fig. 6).

Since CaO has a melting point of 2580°C the substitution of Na^+ ions for Ca^{2+} ions is probably a kinetically controlled phenomenon at 725°C. Thus, the concentration of $[Na^+O^-]$ should be related to the total amount of Na^+, and indeed such was the case as shown in Fig. 2. The equilibrium amount of Na^+ that can be introduced into the CaO crystals is not known; however, samples containing about 2×10^{18} Na^+ ions/g CaO have been prepared by arc melting CaO with an excess of Na_2CO_3 (*13*). This concentration of Na^+ is about two orders of magnitude greater than the maximum concentration of $[Na^+O^-]$ centers observed in this study. There was no observable $[Na^+O^-]$ in the unpromoted CaO, even after heating in O_2.

DISCUSSION

Active Site for the Formation of Methyl Radicals

The data in Fig. 2 imply that a new type of active site for the selective production of

C_2 compounds was generated in CaO upon addition of a sufficient amount of Na_2CO_3 to the oxide. Since the surface area of the promoted CaO was reduced upon introduction of Na_2CO_3, one would expect that the activity of such an oxide would decrease if no new active site were formed in addition to the one already present on the pure oxide. In contrast, the activity of the Na/CaO first increased with Na loading to a maximum (at 15 wt% of Na) and then decreased with further addition of Na^+. The enhanced activity cannot be attributed to the added Na phase, because it was not an active and selective catalyst for the reaction. Therefore, it is more reasonable to suggest that a new active site was created in the Na/CaO catalysts. Since the addition of Na_2CO_3 will result in sintering and the carbonate itself is not active, an excess amount of such material would lower the activity of the catalysts.

For the following reasons, we believed that over the Na/CaO catalysts the selective catalytic site is directly or indirectly (see below) related to the presence of $[Na^+O^-]$ in a manner analogous to the role of $[Li^+O^-]$ in Li/MgO: First, the C_2 yield per unit surface area increased in a parallel manner with the EPR signal intensity of $[Na^+O^-]$. Second, the amount of gas-phase $CH_3\cdot$ radicals generated over Na/CaO and detected by matrix-isolation EPR also varied proportionally with $[Na^+O^-]$ concentration in the catalyst (*17*).

Because of the similarities between $[Na^+O^-]$ and $[Li^+O^-]$ centers, it is reasonable to assume that the mechanism for the formation of $[Na^+O^-]$ should be similar to that of $[Li^+O^-]$ (*10*). The process is summarized by

$$2Na^+O^{2-} + \square + \tfrac{1}{2}O_2 \rightleftarrows 2Na^+O^- + O^{2-} \quad (1)$$

where $\square$ denotes an oxygen ion vacancy. The concentration of $[Na^+O^-]$ depends mainly on the amount of Na^+, the O_2 partial pressure, and the temperature. This center, however, is transient, and rapid quenching is necessary to observe it.

Although $[M^+O^-]$ (M = Group IA ions) centers can always be found in active C_2-producing Group IA/IIA oxide catalysts (*11*), the relationship between the concentration of the centers and activity is not always straightforward. For example, the less active $NaNO_3$/CaO contained a higher concentration of active centers (Table 1), and pure CaO had as great a C_2 selectivity and specific activity as 0.4% Na/CaO (Fig. 2). Oxygen broadening experiments carried out on Na/CaO revealed that only a small fraction of the total $[Na^+O^-]$ centers is in the near-surface region. The remainder are located either in the CaO crystal or buried under the nonactive Na_2CO_3/Na_2O phase (as indicated by XPS results in $NaNO_3$/CaO) where they are not accessible to the gaseous molecules during the broadening experiments and, therefore, catalysis. The existence of such subsurface $[Na^+O^-]$ actually should be expected if the process described by Eq. (1) is operating since a new layer of CaO should be built up on the catalyst surface.

Although alkaline earth oxides are known to be insulators, after promotion with lithium ions the electrical conductivity of MgO was enhanced by a factor of 10^4 compared with the pure material (*18*). Therefore, hole transport is possible and apparently very extensive in this type of promoted oxide. A more precise description of the $[Na^+O^-]$ in Na/CaO at high temperature should be a dynamic equilibrium in which hole transport via O^{2-} ions prevails between $[Na^+O^-]$ and other oxide ions around this center, including those on surface:

$$Na^+O^- + O_s^{2-} \rightleftarrows Na^+O^{2-} + O_s^-. \quad (2)$$

Thus, under reaction conditions a number of surface O_s^- should be available for reacting with CH_4, and their concentration should be proportional to the total concentration of $[Na^+O^-]$ and the exposed CaO surface area.

Although there exists a proportionality between the surface O_s^- concentration and the total $[Na^+O^-]$ concentration, the actual

relationship between the two may depend upon other factors such as the distribution of Na^+ within the crystallite. For example, a greater concentration of the Na^+ in the near-surface region may result in a proportionally greater concentration of O_s^- centers. Thus, the anomaly observed with 0.4% Na/CaO may result from a more homogeneous distribution of Na^+ at this lower loading, i.e., a smaller concentration of $[Na^+O^-]$ in the near-surface region.

The unexpectedly low specific activity of the sample prepared from the $NaNO_3$ (Table 1) may be the result of other factors such as blocking of the active surface by an inactive phase. For instance, sodium nitrate melts at a much lower temperature than the sodium carbonate (305°C versus 851°C) and the XPS data in Table 2 confirm that the concentration of the surface Ca^{2+} is considerably less on the used catalyst prepared from the $NaNO_3$. Although the total surface area of this material is greater, the active surface area apparently is less.

There is considerable evidence that O^- ions, both on the surface and in the gas phase, react with alkanes by hydrogen atom abstraction to produce alkyl radicals (*19–21*). Since $CH_3\cdot$ radicals were also observed over our catalyst, it is reasonable to assume that a similar reaction occurs:

$$CH_4 + O_s^- \rightleftarrows CH_3\cdot + OH_s^- \qquad (3)$$

The surface then dehydroxylates and reacts with O_2 to regenerate the active site O_s^- to complete a catalytic cycle.

$$2OH_s^- \rightarrow O_s^{2-} + \square + H_2O \qquad (4)$$

$$O_s^{2-} + \square + \tfrac{1}{2}O_2 \rightleftarrows 2O_s^- \qquad (5)$$

Since O_s^- can be stabilized on the catalysts, there is clearly another possible regeneration process:

$$2OH_s^- \rightarrow O_s^- + e^- + H_2O \qquad (6)$$

$$e^- + \tfrac{1}{2}O_2 \rightleftarrows O_s^- \qquad (7)$$

It has been shown that O^- on MgO reacts with alkanes at a rate governed by the transport of the hydrocarbon (*19*); thus, reaction (3) probably proceeds very fast during catalysis. Reactions (4) to (7), which involve dehydroxylation of the surface and dissociation of the O–O bond, require high temperatures and are believed to be the rate-controlling steps in our reaction.

The strong influence of O_2 on the increase in the CH_4 conversion (Fig. 6) suggests that adsorption and dissociation of O_2 control the reaction rate at pressures less than 20 Torr. Above 20 Torr of O_2, the availability of O_2 no longer controls the rate, and a zero-order dependence in O_2 on rate is expected. The controlling step, presumably, switches to the dehydroxylation process. The linear increase in $[Na^+O^-]$ concentration in a region of O_2 pressure where the activity goes through a maximum and then is constant at first seems inconsistent. It should be pointed out, however, that the samples used for the EPR experiments were not prepared under catalytic conditions in that no CH_4 was present, and the slow step in the catalytic cycle [reaction (4) or (6)] was not a factor.

When the same experiments were carried out at 675°C to effect the more rapid dehydroxylation process, the amount of CH_4 reacted indeed increased by a factor of 3.8 (29.2 Torr versus 7.7 Torr of CH_4 at 100 Torr of O_2). At this higher temperature, no maximum was observed in the CH_4 conversion region as the O_2 was increased.

The occurrence of the maximum in CH_4 conversion at 625°C and 60 Torr of O_2 is best interpreted by a gas-phase free radical chain mechanism. In addition to the primary channel via the catalyst surface, radical mechanisms involving $CH_3\cdot$ and $CH_3O_2\cdot$ are well known in the gas-phase oxidation of hydrocarbons (*10, 22–25*). One such mechanism is

$$CH_3\cdot + O_2 \rightleftarrows CH_3O_2\cdot \qquad (8)$$

$$CH_3O_2\cdot + C_2H_6 \rightarrow CH_3O_2H + C_2H_5\cdot \qquad (9)$$

$$2CH_3O_2\cdot \rightarrow CH_2O + CH_3OH + O_2 \rightarrow CO, CO_2 \qquad (10)$$

$$CH_3O_2H \rightarrow CH_3O\cdot + OH\cdot \quad (11)$$

$$CH_3O\cdot + CH_4 \rightarrow CH_3OH + CH_3\cdot \quad (12)$$

$$OH\cdot + CH_4 \rightarrow CH_3\cdot + H_2O \quad (13)$$

This mechanism can proceed only when a sufficient concentration of branching reagent, CH_3O_2H, is present [reaction (11)]. Because of its modest reactivity, $CH_3O_2\cdot$ can abstract a hydrogen atom only from a substrate with moderate C–H bond strength such as in C_2H_6 and CH_2O. The C_2H_6 happens to be a product, and its presence will autocatalyze the chain reaction.

Since both $CH_3O_2\cdot$ and C_2H_6 are produced from the $CH_3\cdot$, there should be an optimum O_2 pressure to maximize the CH_3O_2H concentration, and thus, a maximum in the conversion of CH_4 is expected. The maximum activity, however, was not located at 20 Torr of O_2, where the maximum amount of C_2H_6 was obtained. The displacement of the position of the maximum is probably due to the competition between the highly exothermic self-decomposition of $CH_3O_2\cdot$ to C_1 compounds [reaction (10)] with hydrogen atom abstraction [reaction (9)]. This shifts the maximum to 50 Torr of O_2, where a higher steady-state concentration of $CH_3O_2\cdot$ can be obtained, but still enough C_2H_6 is available. In the region after the maximum, intentional addition of C_2H_6 did help to recover the lost activity.

The contribution of chain reactions in our system was not extensive (a maximum of 15% under the conditions of Fig. 6) due to the competition from the more favorable disproportionation reaction of $CH_3O_2\cdot$ (reaction 10) at the lower temperatures. Furthermore, the presence of C_2H_6 is essential for the chain reactions to proceed, and at 200 Torr of O_2, where only a small amount of C_2H_6 was found, the chain reactions were completely terminated as evidenced by the constant CH_4 conversion as the O_2 pressure was increased.

At higher temperatures, which favor formation of more C_2H_6, this chain mechanism may be operating to a greater extent as indicated by the significant increase in CH_4 conversion and the greater C_2H_4-to-C_2H_6 ratio with increasing O_2 pressure (Table III; compare runs 3 and 4, or 6 and 7). However, in this case at least part of the increase must be attributed to an increase in the concentration of $[Na^+O^-]$ centers in the catalysts.

Another significant effect of the chain mechanism is the decomposition reaction of $CH_3O_2\cdot$ to C_1 compounds [reaction (10)] (*26–34*). Contrary to tertiary peroxy radicals, primary peroxy radicals can disproportionate to aldehydes and alcohols rather easily, with the release of a large amount of energy (*30–33*). Since it has already been shown that only a small amount of C_2 is oxidized at 625°C, the formation of C_1 via $CH_3O_2\cdot$ seems to be the best alternative in the lower-temperature range. The $CH_3O_2\cdot$ radicals were observed separately using matrix-isolation EPR (*20, 27*) and mass spectroscopies (*28*), and their concentrations are a strong function of the O_2 pressure and temperature.

Stable Product Formation

One of the most remarkable and significant observations in our study was the increase of C_2 selectivity with temperature up to 675°C. Such an increase is unusual in an oxidation process. A primary reason for the change in product distribution is the reversibility of reaction (8), which is caused by the weak CH_3–O_2 bond. The equilibrium in the gas phase between $CH_3\cdot$ and $CH_3O_2\cdot$ has been measured by Khachatryan *et al.* (*27*) and by Slagle and Gutman (*28*). The data from the former study were extrapolated to high temperatures, and the results are depicted in Fig. 8. Higher temperatures clearly favor the dissociation of $CH_3O_2\cdot$ radicals, and eliminate the production of C_1 through reaction (10). When the CH_4 conversion was limited by the availability of O_2, it was demonstrated over La_2O_3 (which produced more $CH_3\cdot$ radicals than Li/MgO at 600°C) that a decrease in C_1 selectivity was accompanied by an equal increase

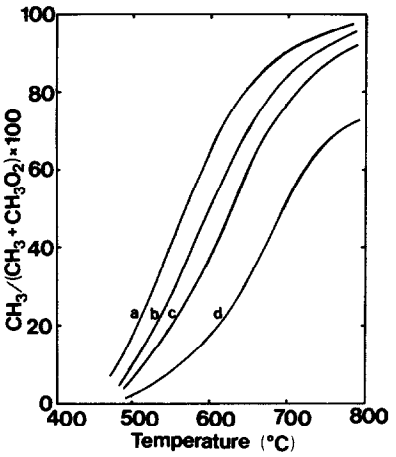

FIG. 8. Gas-phase equilibrium distribution of methyl radicals at various temperatures and oxygen pressures: (a) 20 Torr, (b) 40 Torr, (c) 60 Torr, (d) 200 Torr.

in C_2 selectivity as the temperature was increased.

The effects of temperature and CH_4/O_2 ratio on C_2 selectivity, the evidence for chain reactions, and the observation of gas-phase $CH_3\cdot$ radicals by EPR all suggest that the primary product, C_2H_6, was produced through coupling of two gas-phase $CH_3\cdot$ radicals:

$$2CH_3\cdot \rightleftarrows C_2H_6. \qquad (14)$$

Equation (14) implies that kinetic control of C_2 production is important in determining the C_2 selectivity. Since the rate of formation of C_2 is proportional to the square of $CH_3\cdot$ concentration, C_2 selectivity is favored, up to a point, by more active catalysts and higher temperatures, both of which result in greater $CH_3\cdot$ radical concentrations. The effect of a better catalyst is reflected in the data of Fig. 2, and the effect of temperature in Fig. 4. This kinetic effect also applies to the results in Fig. 5, where at a sufficiently high CH_4 conversion (higher $CH_3\cdot$ concentration) the formation of C_2 instead of C_1 becomes more favorable.

C_2 selectivity also may be influenced by the competitive reaction of $CH_3\cdot$ radicals with the surface, which results in methoxy ions, CH_3O^- [reaction (15)] (*10, 12, 19, 20, 35, 36*). These intermediates can either thermally decompose to CH_2O (*35, 36*) or react with H_2O to produce CH_3OH [reaction (16)] (*12, 37, 38*). Under the reaction conditions employed here these oxygenates were further oxidized to CO and CO_2.

$$CH_3\cdot + O^{2-} \rightarrow CH_3O^- + e^- \qquad (15)$$

$$CH_3O^- \rightarrow CH_3OH,\ CH_2O \rightarrow CO,\ CO_2 \qquad (16)$$

The decrease in CO_2 production with time on stream (Fig. 1) supports the above hypothesis. It is known that prolonged thermal treatment (*39–41*) and the presence of alkali metal ions result in the sintering of alkaline earth metal oxides (*10*). Therefore, C_2 selectivity is obtained only with low-surface-area catalysts. Recently, Aika and coworkers (*6*) studied promoter effects over MgO and likewise concluded that higher C_2 selectivity is favored by lower surface areas.

With an excess amount of CH_4, both C_2H_6 and C_2H_4 produced very small amounts of C_1 compounds over Na/CaO at 625°C (Table 4). However, further oxidation of C_2 is extensive above 675°C (*10*). We believe that the further oxidation proceeds in a consecutive manner,

$$2CH_3\cdot \rightarrow C_2H_6 \rightarrow C_2H_4 \rightarrow CO,\ CO_2 \qquad (17)$$

and there is no evidence to support direct conversion of C_2H_6 into carbon oxides.

At high temperatures and moderate O_2 pressures (e.g., 40 Torr), a considerable amount of C_2H_4 was produced through further oxidation of C_2H_6. We previously proposed that C_2H_6 lost its hydrogen to $[M^+O^-]$ to produce $C_2H_5\cdot$ radicals (*10, 19*), which could react with O^{2-} to give C_2H_4;

$$C_2H_6 + [M^+O^-] \rightarrow C_2H_5\cdot + [M^+OH^-]_s \qquad (18)$$

$$C_2H_5\cdot + O^{2-} \rightarrow C_2H_5O^- + e^- \qquad (19)$$

$$C_2H_5O^- \rightarrow C_2H_4 + OH^-. \qquad (20)$$

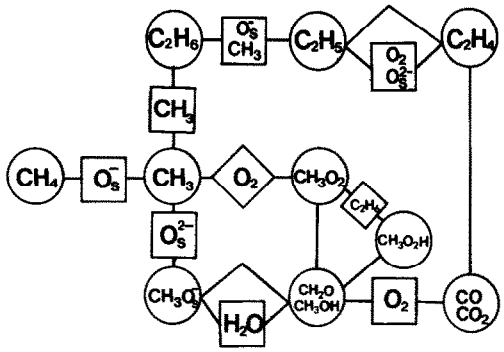

FIG. 9. Reaction scheme summarizing the formation of various products during the oxidative dimerization of methane over Group IA/Group IIA metal oxides.

However, over three totally different catalyst surfaces (Table 1) C_2H_4 to C_2H_6 ratios were all equal to 0.9. This suggests that C_2H_4 formation may also proceed in the gas phase via reactions (9) and (21) to (23). In the presence of O_2, reaction (23) is expected to dominate over reaction (22) in the production of C_2H_4 (*42–46*),

$$CH_3\cdot + C_2H_6 \rightarrow CH_4 + C_2H_5\cdot \quad (21)$$

$$C_2H_5\cdot \rightarrow C_2H_4 + H\cdot \quad (22)$$

$$C_2H_5\cdot + O_2 \rightarrow C_2H_4 + HO_2\cdot \quad (23)$$

CONCLUSIONS

The various aspects of the mechanism proposed in the discussion section are summarized in a scheme depicted in Fig. 9. Obviously the system is complicated because of surface and gas-phase reactions which are coupled by the surface generation of radical intermediates. Nevertheless, the C_2 yields obtained are some of the best which have been reported and the complexity of the system leaves ample opportunity for further optimization.

The study provides further support for the important role of $[M^+O^-]$ centers in the oxidative dimerization of CH_4 over Group IA/IIA oxide catalysts. There is considerable evidence that the reaction is heterogeneous–homogeneous in nature. Methyl radicals are produced by the reaction of CH_4 with surface O_s^- ions, and these radicals then desorb into the gas phase, where they either couple to produce C_2H_6 or react with O_2 to produce oxygenates. The latter is further oxidized to undesirable carbon oxides. The reversible reaction between $CH_3\cdot$ and O_2 influences the catalytic activity and C_2 selectivity. A chain mechanism involving CH_3O_2H as the chain branching reagent is believed to be operating to some degree. Surface reactions between $CH_3\cdot$ and lattice O^{2-} also produce oxygenates as primary products, but again, under the reaction conditions, they are oxidized further. For better C_2 selectivity, a catalyst having low surface area is preferred.

ACKNOWLEDGMENT

This research was supported by the National Science Foundation under Grant CHE-8405191.

REFERENCES

1. Otsuka, K., Jinno, K., and Morikawa, A., *Chem. Lett.*, 499 (1985); *J. Catal.* **100,** 353 (1986).
2. Lin, C.-H., Campbell, K. D., Wang, J.-X., and Lunsford, J. H., *J. Phys. Chem.* **90,** 534 (1986); Campbell, K. D., Zhang, H., and Lunsford, J. H., *J. Phys. Chem.* **92,** 750 (1988).
3. Hinsen, W., Bytyn, W., and Baerns, M., *in* "Proceedings, 8th International Congress on Catalysis, Berlin, July 1984," Vol. III, p. 581. Dechema, Frankfurt, 1984; Bytyn, W., and Baerns, M., *Appl. Catal.* **28,** 199 (1986).
4. Otsuka, K., Liu, Q., Hatano, M., and Morikawa, A., *Chem. Lett.*, 903 (1986); Otsuka, K., Liu, K., Hatano, M., and Morikawa, A., *Chem. Lett.*, 467 (1986); Otsuka, K., Liu, Q., and Morikawa, A. J., *Chem. Soc. Chem. Commun.*, 586 (1986).
5. Ali Emesh, I. T., and Amenomiya, Y., *J. Phys. Chem.* **90,** 4785 (1986).
6. Moriyama, T., Takasaki, N., Iwamatsu, E., and Aika, K., *Chem. Lett.*, 1165 (1986); Iwamatsu, E., Moriyama, T., Takasaki, N., and Aika, K. J., *Chem. Soc. Chem. Commun.*, 19 (1987).
7. Matsuura, I., Utsumi, Y., Nakai, M., and Doi, T., *Chem. Lett.*, 1981 (1986).
8. Jones, C. A., Leonard, J. J., and Sofranko, J. A., *J. Catal.* **103,** 311 (1987).
9. Kimble, J. B., and Kolts, J. H., *Energy Prog.* **6,** 226 (1986); *Chemtech*, 501 (1987).
10. Ito, T., and Lunsford, J. H., *Nature (London)* **314,** 721 (1985). Ito, T., Wang, J.-X., Lin, C.-H., and Lunsford, J. H., *J. Amer. Chem. Soc.* **107,** 5062 (1985).

11. Lin, C.-H., Wang, J.-X., Ito, T., and Lunsford, J. H., *J. Amer. Chem. Soc.* **109,** 4808 (1987).
12. Liu, H.-F., Liu, R.-S., Liew, K.-Y., Johnson, R. E., and Lunsford, J. H., *J. Amer. Chem. Soc.* **106,** 4117 (1984).
13. Tohver, H. T., Henderson, B., Chen, Y., and Abraham, M. M., *Phys. Rev. B* **5,** 3276 (1972).
14. Golodets, E. I., "Heterogeneous Catalytic Reactions Involving Molecular Oxygen." Elsevier, New York, 1982.
15. Boomer, E. H., and Thomas, V., *Canad. J. Res.* **15B,** 401 (1937); **15B,** 414 (1937).
16. Stroud, H. J. F., British Patent 1398385, 1975.
17. Campbell, K. D., and Lunsford, J. H., to be published.
18. Chen, Y., Kernohen, R. H., Boldu, J. L., and Abraham, M. M., *Solid State Commun.* **33,** 441 (1980).
19. Aika, K., and Lunsford, J. H., *J. Phys. Chem.* **81,** 1393 (1977).
20. Driscoll, D. J., Martir, W., Wang, J.-X., and Lunsford, J. H., *J. Amer. Chem. Soc.* **107,** 58 (1985).
21. Bohme, D. K., and Fehsenfeld, F. C., *Canad. J. Chem.* **47,** 2717 (1969).
22. Shtern, V. Ya., "The Gas Phase Oxidation of Hydrocarbons." Butterworths, New York, 1962.
23. Garcia, E. Y., and Loffler, D. G., *Lat. Amer. J. Chem. Eng. Appl. Chem.* **14,** 267 (1984).
24. Benson, S. W., and Nangia, P. S., *Acc. Chem. Res.* **12,** 223 (1979).
25. McKay, G., *Prog. Energy Combust. Sci.* **3,** 105 (1977).
26. Bell, K. M., and Tipper, C. F. H., *Proc. R. Soc. London Ser. A* **238,** 256 (1956).
27. Khachatryan, L. A., Niazyan, O. M., Mantashyan, A. A., Vedeneev, V. I., and Teitel'boim, M. A., *Int. J. Chem. Kinet.* **14,** 1231 (1982).
28. Slagle, I. R., and Gutman, D., *J. Amer. Chem. Soc.* **107,** 5342 (1985).
29. Baldwin, A. C., and Golden, D. M., *Chem. Phys. Lett.,* **55,** (1978).
30. Luckett, G. A., and Mile, B., *Combust. Flame* **26,** 299 (1976).
31. Selby, K., and Waddington, D. J., *J. Chem. Soc. Perkin Trans.* **9,** 1259 (1979).
32. Bartlett, P. D., and Guaraldi, G., *J. Amer. Chem. Soc.* **79,** 3871 (1957).
33. Russell, G. A., *J. Amer. Chem. Soc.* **89,** 4799 (1967).
34. Vardanyan, I. A., Sachyan, G. A., and Nalbandyan, A. B., *Combust. Flame* **17,** 315 (1971).
35. Zhen, K. J., Kahn, M. M., Mak, C. H., Lewis, K. B., and Somorjai, G. A., *J. Catal.* **94,** 501 (1985).
36. Khan, M. M., and Somorjai, G. A., *J. Catal.* **91,** 263 (1985).
37. Bradley, D. C., "Metal Alkoxides." Academic Press, New York, 1978.
38. Bradley, D. C., *Prog. Inorg. Chem.* **2,** 203 (1960).
39. Jones, C. F., Reeve, R. A., Rigg, R., Segall, R. L., Smart, R., and Turner, P., *J. Chem. Soc. Faraday Trans. 1* **80,** 2609 (1984).
40. Kotera, Y., Saito, T., and Terada, M., *Bull. Chem. Soc. Japan* **36,** 195 (1963).
41. Dell, R. M., and Weller, S. W., *Trans. Faraday Soc.* **55,** 2203 (1959).
42. Kulich, D. M., and Taylor, J. E., *Int. J. Chem. Kinet.* **7,** 895 (1975).
43. Taylor, J. E., and Kulich, D. M., *Int. J. Chem. Kinet.* **5,** 455 (1973).
44. Slagle, I. R., Ratajczak, E., and Gutman, D., *J. Phys. Chem.* **90,** 402 (1986).
45. Slagle, I. R., Feng, Q., and Gutman, D., *J. Phys. Chem.* **88,** 3648 (1984).
46. Geisbrecht, R., and Daubert, T. E., *Ind. Eng. Chem. Process Des. Dev.* **14,** 159 (1975).